



## The relationship between white matter microstructure and self-perceived cognitive decline

Derek B. Archer<sup>a,b,c</sup>, Elizabeth E. Moore<sup>a,b</sup>, Ujwala Pamidimukkala<sup>a,b</sup>,  
Niranjana Shashikumar<sup>a,b</sup>, Kimberly R. Pechman<sup>a,b</sup>, Kaj Blennow<sup>g,h,i</sup>, Henrik Zetterberg<sup>g,h,i,j</sup>,  
Bennett A. Landman<sup>d,e,f</sup>, Timothy J. Hohman<sup>a,b,c</sup>, Angela L. Jefferson<sup>a,b,k,\*</sup>, Katherine  
A. Gifford<sup>a,b</sup>

<sup>a</sup> Vanderbilt Memory and Alzheimer's Center, Vanderbilt University Medical Center, Nashville, TN, USA

<sup>b</sup> Department of Neurology, Vanderbilt University Medical Center, Nashville, TN, USA

<sup>c</sup> Vanderbilt Genetics Institute, Vanderbilt University School of Medicine, Nashville, TN, USA

<sup>d</sup> Vanderbilt University Institute of Imaging Science, Vanderbilt University Medical Center, Nashville, TN, USA

<sup>e</sup> Department of Biomedical Engineering, Vanderbilt University, Nashville, TN, USA

<sup>f</sup> Department of Electrical and Computer Engineering, Vanderbilt University, Nashville, TN, USA

<sup>g</sup> Department of Psychiatry and Neurochemistry, Institute of Neuroscience and Physiology, The Sahlgrenska Academy at University of Gothenburg, Mölndal, Sweden

<sup>h</sup> Clinical Neurochemistry Laboratory, Sahlgrenska University Hospital, Mölndal, Sweden

<sup>i</sup> Department of Neurodegenerative Disease, University College London Institute of Neurology, Queen Square, London, England

<sup>j</sup> UK Dementia Research Institute, London, England

<sup>k</sup> Department of Medicine, Vanderbilt University Medical Center, Nashville, TN, USA

### ABSTRACT

Subjective cognitive decline (SCD) is a perceived cognitive change prior to objective cognitive deficits, and although it is associated with Alzheimer's disease (AD) pathology, it likely results from multiple underlying pathologies. We investigated the association of white matter microstructure to SCD as a sensitive and early marker of cognitive decline and quantified the contribution of white matter microstructure separate from amyloidosis. Vanderbilt Memory & Aging Project participants with diffusion MRI data and a 45-item measure of SCD were included [ $n = 236$ , 137 cognitively unimpaired (CU), 99 with mild cognitive impairment (MCI),  $73 \pm 7$  years, 37% female]. A subset of participants (64 CU, 40 MCI) underwent a fasting lumbar puncture for quantification of cerebrospinal fluid (CSF) amyloid- $\beta$  (CSF A $\beta_{42}$ ), total tau (CSF t-tau), and phosphorylated tau (CSF p-tau). Diffusion MRI data was post-processed using the free-water (FW) elimination technique, which allowed quantification of extracellular (FW) and intracellular compartment (fractional anisotropy, mean diffusivity, axial diffusivity, and radial diffusivity) microstructure. Microstructural values were quantified within 11 cognitive-related white matter tracts, including medial temporal lobe, frontal transcallosal, and fronto-parietal tracts using a region of interest approach. General linear modeling related each tract to SCD scores adjusting for age, sex, race/ethnicity, education, Framingham Stroke Risk Profile scores, APOE  $\epsilon 4$  carrier status, diagnosis, Geriatric Depression Scale scores, hippocampal volume, and total white matter volume. Competitive models were analyzed to determine if white matter microstructural values have a unique role in SCD scores separate from CSF A $\beta_{42}$ . FW-corrected radial diffusivity (RD<sub>T</sub>) was related to SCD scores in 8 tracts: cingulum bundle, inferior longitudinal fasciculus, as well as inferior frontal gyrus (IFG) pars opercularis, IFG orbitalis, IFG pars triangularis, tapetum, medial frontal gyrus, and middle frontal gyrus transcallosal tracts. While CSF A $\beta_{42}$  was related to SCD scores in our cohort ( $R_{adj}^2 = 39.03\%$ ;  $\beta = -0.231$ ;  $p = 0.020$ ), competitive models revealed that fornix and IFG pars triangularis transcallosal tract RD<sub>T</sub> contributed unique variance to SCD scores beyond CSF A $\beta_{42}$  ( $R_{adj}^2 = 44.35\%$  and  $R_{adj}^2 = 43.09\%$ , respectively), with several other tract measures demonstrating nominal significance. All tracts which demonstrated nominal significance (in addition to covariates) were input into a backwards stepwise regression analysis. ILF RD<sub>T</sub>, fornix RD<sub>T</sub>, and UF FW were best associated with SCD scores ( $R_{adj}^2 = 46.69\%$ ;  $p = 6.37 \times 10^{-12}$ ). Ultimately, we found that medial temporal lobe and frontal transcallosal tract microstructure is an important driver of SCD scores independent of early amyloid deposition. Our results highlight the potential importance of abnormal white matter diffusivity as an early contributor to cognitive decline. These results also highlight the value of incorporating multiple biomarkers to help disentangle the mechanistic heterogeneity of SCD as an early stage of cognitive decline.

\* Corresponding author at: Department of Neurology, Vanderbilt University Medical Center, 1207 17th Avenue South, Suite 204, Nashville, TN 37212, USA.  
E-mail address: [angela.jefferson@vumc.org](mailto:angela.jefferson@vumc.org) (A.L. Jefferson).

<https://doi.org/10.1016/j.nicl.2021.102794>

Received 24 March 2021; Received in revised form 12 August 2021; Accepted 13 August 2021

Available online 28 August 2021

2213-1582/© 2021 The Authors. Published by Elsevier Inc. This is an open access article under the CC BY license (<http://creativecommons.org/licenses/by/4.0/>).

## 1. Introduction

Subjective cognitive decline (SCD) is an individual's self-report of decline or change to cognition (Jessen et al., 2014) and is thought to occur prior to the onset of objective cognitive deficits (Sperling et al., 2011). SCD is a measure which can be reliably measured and is associated with future cognitive changes (Gifford et al., 2014) and conversion to dementia (Gifford et al., 2014), suggesting it may be one of the earliest detectable changes of unhealthy brain aging. SCD is associated with Alzheimer's disease (AD) neuroimaging biomarkers (Lin et al., 2019) (e.g., temporal lobe cortical thinning, (Verfaillie et al., 2018; Meiberth et al., 2015) smaller hippocampal volume (van der Flier et al., 2004; Cherbuin et al., 2015)) and greater SCD is also associated with increased amyloid- $\beta$  ( $A\beta$ ) load (Verfaillie et al., 2019; Perrotin et al., 2017). While SCD may be relevant in early AD, SCD is a heterogeneous construct, likely representing the culmination of many etiologies (Perrotin et al., 2017).

Abnormal white matter microstructure, particularly in the medial temporal lobe projections and frontal lobe tracts, is associated with SCD, with prior literature emphasizing contributions of hippocampal projections, forceps minor, forceps major, the inferior longitudinal fasciculus, and the cingulum bundle (Luo et al., 2019; Ohlhauser et al., 2019). Individuals with SCD have white matter microstructural damage similar to patients with mild cognitive impairment (MCI) (Luo et al., 2019) and diffusion MRI metrics may be more sensitive to SCD than volumetric analyses (Ryu et al., 2017). White matter abnormalities may precede atrophic processes, (Metzler-Baddeley et al., 2019; Bartzokis, 2011) represent a more sensitive marker of early clinical symptoms, (Selnes et al., 2013) and are associated with multiple injury pathways in aging (e.g., cerebrovascular disease) (de Groot et al., 2015). Thus, white matter integrity may be a suitable biomarker for SCD.

However, conventional diffusion MRI techniques have limitations, (Jones et al., 2013) such as partial volume effects, (Pasternak et al., 2009; Alexander et al., 2001) making it difficult to distinguish between intracellular and extracellular compartments. New post-processing techniques, (Pasternak et al., 2009; Pasternak et al., 2012) such as free-water (FW) elimination, separate the diffusion MRI image into intracellular and extracellular compartments. Specifically, the FW-elimination technique is a validated technique which uses a bi-tensor mathematical framework to estimate the proportion of each voxel which has unrestricted diffusion. This proportion of the voxel is then removed from the voxel to provide more accurate assessments of the underlying tissue. Increases in the extracellular compartment are thought to be related to inflammation, atrophy, and edema, while alterations of the intracellular component are thought to be associated with tissue degeneration (Pasternak et al., 2009; Gullett et al., 2020; Pasternak et al., 2016). Using this technique, reductions in white matter microstructure have been associated with higher levels of AD pathology in preclinical AD (Hoy et al., 2017) and were more closely associated with AD pathology than conventional diffusion MRI metrics (Walsh et al., 2020). Finally, our group recently demonstrated that FW-corrected measures interacted with hippocampal atrophy to predict more rapid rates of cognitive decline (Archer et al., 2020). While FW-corrected metrics have been leveraged to evaluate several aspects of objective cognitive decline, they have not yet been used to assess SCD.

The purpose of this study is to use FW post-processing techniques to investigate the associations between white matter microstructure and SCD scores among older adults without clinical dementia. We therefore evaluated white matter tracts which have demonstrated an association with cognitive impairment, which include those projecting from the prefrontal cortex and medial temporal lobe. The involvement of these tracts may arise from a variety of factors, including normal aging, AD, and other pathologies (e.g., vascular disease) (Luo et al., 2019; Ohlhauser et al., 2019; Archer et al., 2020; Archer et al., 2019). These tracts included five medial temporal lobe projections (cingulum bundle, tapetum, fornix, uncinate fasciculus, inferior longitudinal fasciculus),

one fronto-parietal association tract (superior longitudinal fasciculus), and five frontal homologous transcallosal tracts (medial frontal gyrus, middle frontal gyrus, and inferior frontal gyrus pars opercularis, orbitalis, and triangularis). We then quantified FW-corrected metrics within these tracts, including fractional anisotropy ( $FA_T$ ), mean diffusivity ( $MD_T$ ), axial diffusivity ( $AD_T$ ), and radial diffusivity ( $RD_T$ ) using a region-of-interest (ROI) based approach. These microstructural metrics were associated with SCD scores derived from a 45-item questionnaire of self-reported cognitive decline considered on a continuous spectrum (Gifford et al., 2015). We hypothesized that abnormalities in white matter tract diffusivity would be associated with higher SCD scores. We also examined whether these metrics were independently associated with SCD scores beyond CSF  $A\beta_{42}$ . Finally, multivariate regression was conducted to determine the subset of variables which was most associated with SCD scores.

## 2. Materials & methods

### 2.1. Study cohort

Data were drawn from the baseline cohort of the Vanderbilt Memory & Aging Project (VMAP), which is a longitudinal observational study of 335 individuals without dementia launched in 2012 and described elsewhere (Jefferson et al., 2016). Briefly, inclusion criteria for VMAP required participants to be 60 years of age and older, speak English, have adequate auditory/visual acuity, and have a dependable study partner. Participants underwent a neuropsychological assessment for cognitive diagnosis by consensus. Specifically, participants were considered cognitively unimpaired (CU) if they had a Clinical Dementia Rating (CDR) scale score equal to 0, no deficits in activities of daily living attributable to cognitive impairment, (Pfeffer et al., 1982) and had neuropsychological impairment scores within 1.5 standard deviations of the age-adjusted normative mean. In contrast, individuals were considered to have mild cognitive impairment (MCI) if they had a (1) a CDR score  $\geq 0.5$ , (2) relatively spared activities of daily living, (3) neuropsychological performance more than 1.5 standard deviations from the group neuropsychological performance mean in at least one cognitive domain, (4) concern of a cognitive change by the individual, an informant, or a clinician, and (5) absence of dementia (Morris, 1993; Albert et al., 2011). Participants were excluded from the VMAP cohort for a variety of well-defined reasons, including contraindication for 3 T MRI, a history of other neurological disorders (e.g., dementia, stroke, major psychiatric illness), heart failure, head injury with 5 min or more of unconsciousness, and systemic or terminal illness. In the present study, participants were also excluded if they were missing covariates, SCD assessment, or diffusion MRI data, resulting in a sample of 236 individuals in our primary analysis (137 CU, 99 MCI). Further, we conducted an analysis leveraging cerebrospinal fluid in our cohort. In this analysis, there were 104 individuals (64 CU, 40 MCI). The protocol was approved by the Vanderbilt University Medical Center Institutional Review Board, and written informed consent was obtained prior to data collection for all participants.

### 2.2. Subjective cognitive decline (SCD) assessment

Participants completed four SCD questionnaires: the Everyday Cognition Questionnaire (Farias et al., 2008), the Memory Functioning Questionnaire (Gilewski et al., 1990), the Cognitive Changes Questionnaire (Farias et al., 2008; Gilewski et al., 1990; Crook, 1983; Reid and MacLulich, 2006), and the Cognitive Difficulties Scale (Crook, 1983). Items from these questionnaires were reduced into a 45-item questionnaire (Vanderbilt SCD Questionnaire) using factor analytic models (Gifford et al., 2015). Total score on this measure ranges from 5 to 174, with higher scores representing more SCD. This study considered the SCD score as a continuous marker of subjective cognitive experience, rather than a dichotomized diagnostic status. We considered SCD status

across the cognitive spectrum, including CU and MCI individuals (Gifford et al., 2015). Moreover, this score can be partitioned into three subscores: memory, executive function, and language.

### 2.3. Diffusion MRI acquisition and preprocessing

Diffusion images (resolution: 2 mm isotropic,  $b$ -values: 0, 1000 s/mm<sup>2</sup>) were collected along 32 diffusion gradient vectors and 1 B<sub>0</sub> weighted image. FSL 5.0.9 (fsl.fmrib.ox.ac.uk) was used for all diffusion MRI preprocessing (Jenkinson et al., 2012). Quality assessment of all diffusion MRI scans was performed manually. Data were first corrected for head motion and eddy currents and the brain was then extracted from the skull (Smith, 2002; Andersson and Sotiropoulos, 2016). This corrected image was then inputted into custom written MATLAB (R2019a; The MathWorks, Natick, MA) to calculate free-water corrected fractional anisotropy (FA<sub>T</sub>), mean diffusivity (MD<sub>T</sub>), axial diffusivity (AD<sub>T</sub>), radial diffusivity (RD<sub>T</sub>), and FW maps, as previously described (Archer et al., 2020; Archer et al., 2019). The diffusion images were then standardized to the Montreal Neurological Institute (MNI) space using the FA<sub>T</sub> maps. Specifically, the FA<sub>T</sub> map was registered to an in-house template (1 mm isotropic) by a non-linear warp using the Advanced Normalization Tools (ANTs) package (Avants et al., 2008). Normalization accuracy was assessed manually. This non-linear warp was then applied to the MD<sub>T</sub>, AD<sub>T</sub>, RD<sub>T</sub>, and FW maps.

A set of 11 white matter tractography templates in MNI space were collated from several well-established templates, (Archer et al., 2020; Brown et al., 2017; DeSimone et al., 2019) and included medial temporal lobe projections, frontal transcallosal tracts, and fronto-parietal association tracts (Fig. 1). Frontal transcallosal tracts included homologous connections of the inferior frontal gyrus (IFG) pars opercularis, orbitalis, and triangularis as well as inferior temporal gyrus (i.e., tapetum), medial frontal gyrus, and middle frontal gyrus. The fronto-parietal association tract included the superior longitudinal fasciculus (SLF). Medial temporal projections included the cingulum bundle, fornix, inferior longitudinal fasciculus (ILF), and uncinate fasciculus (UF). Using a region-of-interest (ROI) based approach, FA<sub>T</sub>, MD<sub>T</sub>, AD<sub>T</sub>,

RD<sub>T</sub>, and FW metrics were calculated within all 11 tracts for all participants, resulting in a total of 55 values for each participant.

### 2.4. Cerebrospinal fluid acquisition

A subset of participants completed a fasting lumbar puncture ( $n = 104$ ). CSF was collected with polypropylene syringes using a Sprotte 25-gauge spinal needle in an intervertebral lumbar space. Samples were immediately mixed and centrifuged, and supernatants were aliquoted in 0.5 mL polypropylene tubes and stored at  $-80^{\circ}\text{C}$ . Samples were analyzed in batch using commercially available enzyme-linked immunosorbent assays (Fujirebio, Ghent, Belgium) to determine the levels of A $\beta$ <sub>42</sub> (INNOTEST  $\beta$ -AMYLOID<sub>(1-42)</sub>), p-tau (INNOTEST PHOSPHO-TAU<sub>(181P)</sub>), and t-tau (INNOTEST hTAU) (Osborn et al., 2018). Board-certified laboratory technicians processed data blinded to clinical information, as previously described (Palmqvist et al., 2014).

### 2.5. Analytical plan

Covariates included age, sex, race/ethnicity, education, Framingham Stroke Risk Profile (FSRP) Score, (Wolf et al., 1991; D'Agostino et al., 1994) apolipoprotein E (APOE- $\epsilon$ 4) carrier status, diagnosis, and Geriatric Depression Score (GDS) (Yesavage, 1988). Given that we were interested in the association of white matter and SCD scores beyond that of AD contributors, we also adjusted our models for hippocampal volume using established procedures (Archer et al., 2020). Finally, since the temporal ordering of gray and white matter volume loss is currently unclear (Sachdev et al., 2013), we included a white matter volume covariate. APOE- $\epsilon$ 4 genotype status ( $\epsilon$ 2,  $\epsilon$ 3,  $\epsilon$ 4) was determined using single-nucleotide polymorphisms rs7412 and rs429358, which were genotyped using a TaqMan from DNA extracted from frozen whole blood (Jefferson et al., 2016). APOE- $\epsilon$ 4 carrier status was defined as positive ( $\epsilon$ 2/ $\epsilon$ 4,  $\epsilon$ 3/ $\epsilon$ 4,  $\epsilon$ 4/ $\epsilon$ 4) or negative ( $\epsilon$ 2/ $\epsilon$ 2,  $\epsilon$ 3/ $\epsilon$ 3,  $\epsilon$ 2/ $\epsilon$ 3). For primary models, the effect of each tract (IFG pars opercularis, IFG pars orbitalis, IFG pars triangularis, tapetum, medial frontal gyrus, middle frontal gyrus, cingulum bundle, fornix, ILF, SLF, and UF) for all five measures

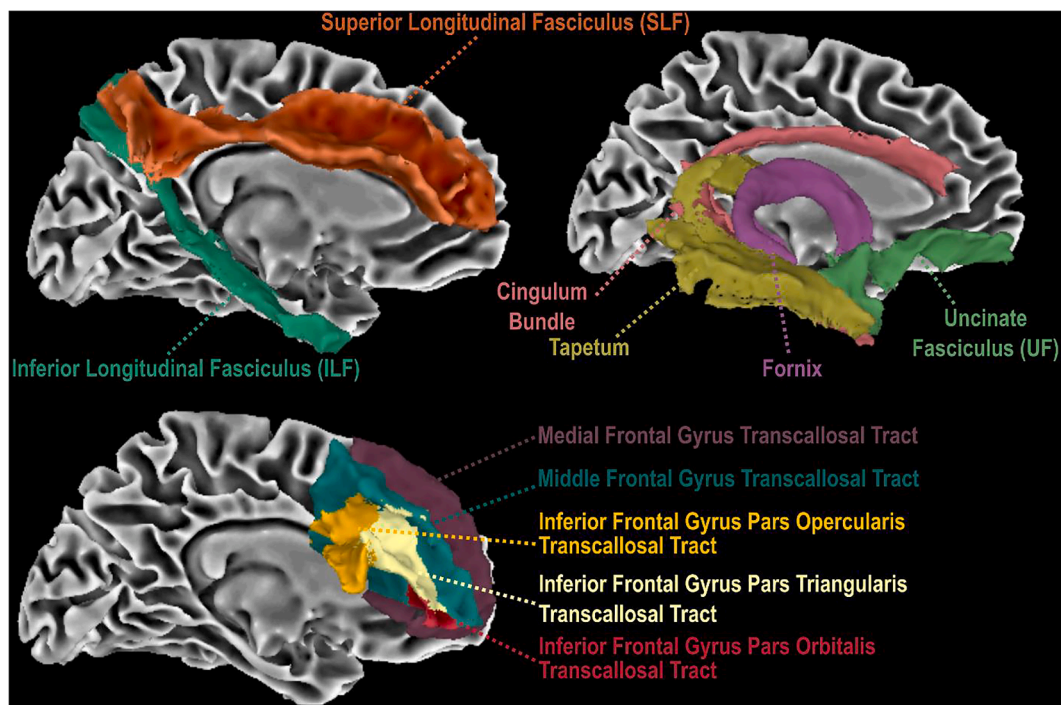


**Fig. 1. Tractography Templates Used in Study.** This study used several previously developed tractography templates to evaluate tract microstructure. All tractography templates are freely available at: [https://github.com/VUMC-VMAC/Tractography\\_Templates](https://github.com/VUMC-VMAC/Tractography_Templates). (Archer et al., 2020; Archer et al., 2019; Brown et al., 2017).



(FA<sub>T</sub>, MD<sub>T</sub>, AD<sub>T</sub>, RD<sub>T</sub>, and FW) on total SCD score was estimated using a general linear model adjusting for all covariates. For each analysis, only one tract per model was considered, and models were standardized to allow easy comparison of beta-coefficients between microstructural measures. Next, the association between CSF Aβ<sub>42</sub> and SCD scores was estimated using a general linear model adjusting for all covariates in a subset of our cohort which had both diffusion MRI and CSF Aβ<sub>42</sub> data (n = 104; 64 CU, 40 MCI). Secondary analyses were conducted to determine if diffusion MRI and CSF measures interacted on SCD scores.

In a separate analysis in the CSF cohort, we then iteratively added each white matter tract metric to determine if unique variance was provided above and beyond covariates and CSF Aβ<sub>42</sub> measures (i.e., a competitive model analysis). Following this analysis, we collated variables which significantly added unique variance above and beyond CSF Aβ<sub>42</sub> and conducted a multivariate regression analysis. Specifically, these input variables (in addition to covariates) were inputted into a backwards stepwise regression analysis to determine the set of variables which maximized the R<sub>adj</sub><sup>2</sup>. In the case where RD<sub>T</sub> and MD<sub>T</sub> were significant for a particular tract, the MD<sub>T</sub> measure was excluded to avoid collinearity. Significance was set a priori as α = 0.05 and correction for multiple comparisons were made using the false discovery rate (FDR) method across all tracts for each measure. All statistical analyses were performed in R version 3.5.2. (<http://www.r-project.org/>).

### 3. Results

#### 3.1. Participant characteristics

Demographic and clinical information for each group (CU, MCI) are summarized in Table 1. As expected, the MCI group had lower MoCA scores and higher SCD scores compared to the cognitively unimpaired group. The MCI group had higher SCD scores, and these findings were consistent across all subscores of SCD (i.e., executive function, language, memory). CSF biomarker data for the CSF cohort (n = 104) is also shown in Table 1. The MCI group had significantly lower CSF Aβ<sub>42</sub> and higher CSF t-tau. There were no between group differences in CSF p-tau. Demographic and clinical information for the CSF cohort can be found in Supplemental Table 1.

#### 3.2. White matter tract microstructure association with subjective cognitive decline scores

The association of FW and FW-corrected white matter tract microstructure (FW, FA<sub>T</sub>, MD<sub>T</sub>, AD<sub>T</sub>, RD<sub>T</sub>) with SCD scores are presented in Table 2 and illustrated in Fig. 2. For FW, there were no significant associations which survived multiple correction. For FA<sub>T</sub>, significant associations were found for the cingulum bundle, ILF, IFG pars orbitalis, IFG pars triangularis, medial frontal gyrus, middle frontal gyrus, SLF, and UF. For MD<sub>T</sub>, there were no significant associations which survived multiple correction. Higher RD<sub>T</sub> in the cingulum bundle, ILF, IFG pars opercularis, IFG pars orbitalis, IFG pars triangularis, tapetum, medial frontal gyrus, and middle frontal gyrus was significantly associated with higher SCD scores. Secondary analyses were conducted to determine the association of tract measures with each SCD subscore. These findings can be found in Supplemental Tables 2-4 and demonstrate that memory and executive function subscores are largely similar to total SCD score associations; in contrast, associations with language were less significant. Further, we conducted an analysis to determine if diffusion MRI and CSF biomarkers interacted on SCD scores. No significant associations were found.

#### 3.3. CSF Aβ<sub>42</sub> and white matter tract microstructure as competitive predictors of subjective cognitive decline scores

The main effect analyses were followed up with analyses in a subset of our cohort which had both diffusion MRI and CSF Aβ<sub>42</sub> data (n = 104).

**Table 1**  
Participant Demographic and Clinical Characteristics.

| Measure                                    | Cognitive Status |                             |            | Test Statistic         | p-value |
|--|------------------|-----------------------------|------------|------------------------|---------|
|  | All              | Cognitively Unimpaired (CU) | MCI        |                        |         |
| <i>Demographics</i>                        |                  |                             |            |                        |         |
| Sample size                                | 236              | 137                         | 99         | –                      | –       |
| Age (years)                                | 73 (7)           | 73 (7)                      | 73 (8)     | t = 0.794              | 0.480   |
| Sex (% male)                               | 63               | 64                          | 62         | χ <sup>2</sup> = 0.075 | 0.784   |
| Education (years)                          | 16 (3)           | 16 (3)                      | 15 (3)     | t = 3.680              | <0.001  |
| Race (% Non-Hispanic white)                | 86               | 85                          | 88         | χ <sup>2</sup> = 0.127 | 0.722   |
| <i>Clinical Characteristics</i>            |                  |                             |            |                        |         |
| MoCA                                       | 25 (3)           | 27 (2)                      | 23 (3)     | H = 72.786             | <0.001  |
| APOE ε4 (% positive)                       | 35               | 41                          | 30         | χ <sup>2</sup> = 2.857 | 0.096   |
| FSRP Score <sup>a</sup>                    | 12 (4)           | 12 (4)                      | 13 (4)     | t = 1.248              | 0.213   |
| Systolic Blood Pressure (mmHg)             | 142 (18)         | 141 (18)                    | 145 (19)   | t = 1.522              | 0.129   |
| Prevalent CVD (%)                          | 5                | 5                           | 3          | χ <sup>2</sup> = 0.486 | 0.486   |
| GDS Score <sup>b</sup>                     | 2 (3)            | 2 (2)                       | 3 (3)      | H = 17.476             | <0.001  |
| Hippocampal Volume (mm <sup>3</sup> )      | 7228 (767)       | 7459 (676)                  | 6907 (773) | t = 5.817              | <0.001  |
| <i>CSF Biomarkers<sup>c</sup></i>          |                  |                             |            |                        |         |
| Aβ <sub>42</sub> (pg/mL)                   | 706 (241)        | 760 (231)                   | 620 (234)  | t = 2.996              | 0.003   |
| T-tau (pg/mL)                              | 422 (212)        | 383 (180)                   | 486 (244)  | H = 4.416              | 0.036   |
| P-tau (pg/mL)                              | 61 (26)          | 57 (22)                     | 67 (29)    | H = 2.573              | 0.109   |
| <i>Subjective Cognitive Decline Scores</i> |                  |                             |            |                        |         |
| Total Score                                | 62 (23)          | 52 (17)                     | 75 (22)    | H = 57.613             | <0.001  |
| Executive Function                         | 11 (5)           | 9 (4)                       | 14 (6)     | H = 40.988             | <0.001  |
| Language                                   | 14 (6)           | 12 (4)                      | 17 (7)     | H = 44.076             | <0.001  |
| Memory                                     | 37 (13)          | 32 (10)                     | 44 (12)    | H = 8.686              | <0.001  |

Values denoted as mean (standard deviation) or frequency. Abbreviations: MoCA, Montreal Cognitive Assessment; APOE ε4, apolipoprotein E ε4; CVD, cardiovascular disease; FSRP, Framingham Stroke Risk Profile; GDS, Geriatric Depression Scale; MCI, mild cognitive impairment. p-values (p < 0.05 bolded) were generated using a one-way analysis of variance for continuous variables and a chi-square test for categorical variables. <sup>a</sup>A modified FSRP score was included in statistical models excluding points assigned to age. <sup>b</sup>GDS score minus points from items 14, 26, 29, and 30. The adjusted range of this score is 0–26. <sup>c</sup>A subset of 104 participants (64 CU, 40 MCI) had CSF biomarker data. Bolded values indicate p < 0.05.

We recapitulate previous findings (Stomrud et al., 2007); (Wolfsgruber et al., 2015) by demonstrating that CSF Aβ<sub>42</sub> is associated with SCD scores (β = −0.231, p = 0.020), whereas t-tau (β = 0.138, p = 0.122) and p-tau (β = 0.129, p = 0.141) are not associated with SCD scores. Therefore, we further assessed white matter associations above and beyond the established associations with CSF Aβ<sub>42</sub> (Table 3). The base model (i.e., CSF Aβ<sub>42</sub> and all covariates) explained 39.03% of the variance to SCD scores (p = 1.78 × 10<sup>−8</sup>). White matter tract microstructural measures were then iteratively added to this model. We found that the fornix MD<sub>T</sub>, fornix RD<sub>T</sub>, and IFG pars triangularis RD<sub>T</sub> contributed

**Table 2**  
White Matter Tract Microstructure Associations with Subjective Cognitive Decline.

|  | Cingulum Bundle | Fornix | ILF           | IFG Pars Opercularis | IFG Pars Orbitalis | IFG Pars Triangularis | Tapetum       | Medial Frontal Gyrus | Middle Frontal Gyrus | SLF           | UF            |
|--|-----------------|--------|---------------|----------------------|--------------------|-----------------------|---------------|----------------------|----------------------|---------------|---------------|
| <i>Free-water (FW)</i>                                     |                 |        |               |                      |                    |                       |               |                      |                      |               |               |
| $\beta$  | 0.043           | 0.009  | 0.058         | 0.069                | 0.105              | 0.062                 | 0.084         | 0.127                | 0.091                | 0.066         | 0.140         |
| $\beta_{SE}$   | 0.074           | 0.071  | 0.071         | 0.068                | 0.067              | 0.067                 | 0.065         | 0.062                | 0.068                | 0.065         | 0.067         |
| <b>p-value</b>   | 0.565           | 0.901  | 0.410         | 0.314                | 0.116              | 0.355                 | 0.202         | <b>0.042</b>         | 0.184                | 0.306         | <b>0.037</b>  |
| $f^2$  | 0.001           | 0.000  | 0.003         | 0.005                | 0.011              | 0.004                 | 0.007         | 0.019                | 0.008                | 0.005         | 0.020         |
| <i>FW-corrected fractional anisotropy (FA<sub>T</sub>)</i> |                 |        |               |                      |                    |                       |               |                      |                      |               |               |
| $\beta$  | -0.168          | 0.000  | -0.186        | -0.146               | -0.136             | -0.153                | -0.115        | -0.153               | -0.150               | -0.121        | -0.139        |
| $\beta_{SE}$   | 0.058           | 0.062  | 0.058         | 0.053                | 0.057              | 0.054                 | 0.057         | 0.059                | 0.055                | 0.055         | 0.057         |
| <b>p-value</b>   | <b>0.004*</b>   | 1.000  | <b>0.001*</b> | <b>0.007</b>         | <b>0.018*</b>      | <b>0.005*</b>         | <b>0.043</b>  | <b>0.011*</b>        | <b>0.007*</b>        | <b>0.028*</b> | <b>0.016*</b> |
| $f^2$  | 0.037           | 0.000  | 0.046         | 0.033                | 0.025              | 0.035                 | 0.018         | 0.030                | 0.033                | 0.022         | 0.026         |
| <i>FW-corrected mean diffusivity (MD<sub>T</sub>)</i>      |                 |        |               |                      |                    |                       |               |                      |                      |               |               |
| $\beta$  | 0.154           | 0.067  | 0.114         | 0.112                | 0.035              | 0.118                 | 0.082         | 0.143                | 0.106                | 0.038         | 0.034         |
| $\beta_{SE}$   | 0.055           | 0.067  | 0.053         | 0.056                | 0.054              | 0.056                 | 0.055         | 0.052                | 0.056                | 0.055         | 0.057         |
| <b>p-value</b>   | <b>0.005</b>    | 0.314  | <b>0.033</b>  | <b>0.047</b>         | 0.520              | <b>0.038</b>          | 0.134         | <b>0.007</b>         | 0.060                | 0.492         | 0.550         |
| $f^2$  | 0.035           | 0.005  | 0.020         | 0.018                | 0.002              | 0.020                 | 0.010         | 0.033                | 0.016                | 0.002         | 0.002         |
| <i>FW-corrected axial diffusivity (AD<sub>T</sub>)</i>     |                 |        |               |                      |                    |                       |               |                      |                      |               |               |
| $\beta$  | -0.080          | 0.010  | -0.114        | -0.075               | -0.119             | -0.106                | -0.038        | -0.096               | -0.100               | -0.100        | -0.115        |
| $\beta_{SE}$   | 0.065           | 0.065  | 0.061         | 0.055                | 0.054              | 0.056                 | 0.055         | 0.057                | 0.055                | 0.058         | 0.061         |
| <b>p-value</b>   | 0.220           | 0.878  | 0.061         | 0.171                | <b>0.029</b>       | 0.058                 | 0.492         | 0.093                | 0.072                | 0.087         | 0.061         |
| $f^2$  | 0.007           | 0.000  | 0.016         | 0.008                | 0.021              | 0.016                 | 0.002         | 0.013                | 0.015                | 0.013         | 0.016         |
| <i>FW-corrected radial diffusivity (RD<sub>T</sub>)</i>    |                 |        |               |                      |                    |                       |               |                      |                      |               |               |
| $\beta$  | 0.181           | 0.075  | 0.173         | 0.148                | 0.136              | 0.161                 | 0.121         | 0.175                | 0.154                | 0.087         | 0.110         |
| $\beta_{SE}$   | 0.052           | 0.060  | 0.053         | 0.054                | 0.053              | 0.052                 | 0.053         | 0.053                | 0.053                | 0.053         | 0.054         |
| <b>p-value</b>   | <b>0.001*</b>   | 0.211  | <b>0.001*</b> | <b>0.006*</b>        | <b>0.010*</b>      | <b>0.002*</b>         | <b>0.024*</b> | <b>0.001*</b>        | <b>0.004*</b>        | 0.100         | <b>0.042</b>  |
| $f^2$  | 0.054           | 0.007  | 0.047         | 0.034                | 0.030              | 0.042                 | 0.023         | 0.048                | 0.038                | 0.012         | 0.019         |

FW-corrected metrics were associated with SCD in 236 participants (137 CU, 99 MCI). Abbreviations: IFG, inferior frontal gyrus; ILF, inferior longitudinal fasciculus; SLF, superior longitudinal fasciculus; UF, uncinate fasciculus;  $\beta$ , beta-coefficient for variable of interest;  $\beta_{SE}$ , standard error of the beta-coefficient. Bolded values indicate  $p < 0.05$ ,  $*p_{FDR} < 0.05$ .

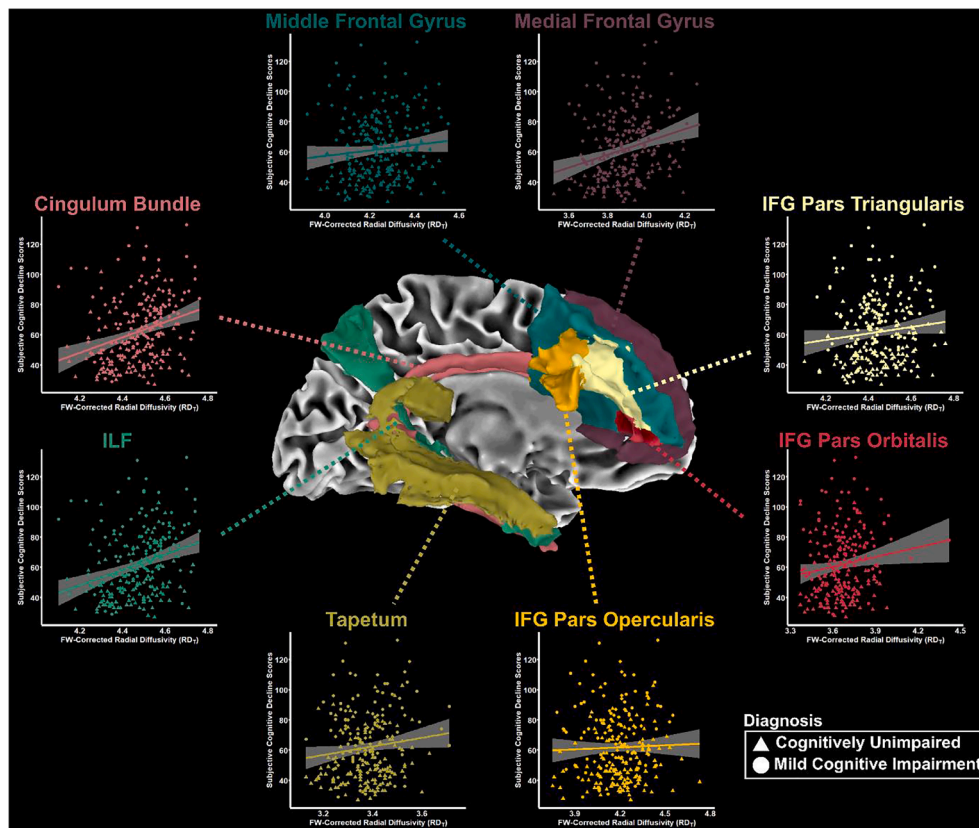


**Fig. 2.**  $RD_T$  Associations with Subjective Cognitive Decline (SCD) scores. (A)  $RD_T$  within the cingulum bundle, medial frontal gyrus, middle frontal gyrus, inferior longitudinal fasciculus (ILF), IFG pars triangularis, IFG pars orbitalis, IFG pars opercularis, and tapetum were significant predictors of subjective cognitive decline. (B) Solid lines reflect fitted regressions with tract  $RD_T$  and SCD. Shading reflects 95% CI.

**Table 3**  
Competitive Models of White Matter Microstructure and Amyloidosis with Subjective Cognitive Decline.

| Model                            | $\Delta R_{adj}^2$ |                 |                 |                 |                 |
|----------------------------------|--------------------|-----------------|-----------------|-----------------|-----------------|
|                                  | FW                 | FA <sub>T</sub> | MD <sub>T</sub> | AD <sub>T</sub> | RD <sub>T</sub> |
| Cingulum Bundle                  | -0.481             | 1.581           | 0.802           | -0.195          | 1.854           |
| Fornix                           | 0.613              | -0.003          | <b>5.438*</b>   | 0.977           | <b>5.318*</b>   |
| ILF                              | -0.226             | 1.440           | 0.728           | 0.303           | <b>2.389</b>    |
| IFG Pars Opercularis             | -0.327             | 0.497           | <b>2.523</b>    | -0.571          | <b>1.965</b>    |
| IFG Pars Orbitalis               | -0.328             | 1.640           | -0.455          | 1.421           | <b>2.310</b>    |
| IFG Pars Triangularis            | -0.558             | 1.541           | <b>3.523</b>    | 0.068           | <b>4.058*</b>   |
| Tapetum                          | -0.015             | 0.021           | 1.806           | -0.536          | <b>2.229</b>    |
| Medial Frontal Gyrus             | -0.160             | 0.188           | <b>2.321</b>    | -0.091          | <b>2.269</b>    |
| Middle Frontal Gyrus             | -0.222             | 1.695           | 1.546           | 0.616           | <b>2.931</b>    |
| Superior Longitudinal Fasciculus | -0.592             | 0.336           | -0.645          | 0.065           | -0.208          |
| Uncinate Fasciculus              | <b>2.323</b>       | 0.379           | -0.413          | 0.676           | -0.346          |

The baseline model (CSF  $A\beta_{42}$  and all covariates) explained 39.03% of the variance to SCD in 104 participants (64 CU, 40 MCI). White matter tract microstructural values were then iteratively added to this base model and the  $R_{adj}^2$  values were compared. The table shows the  $\Delta R_{adj}^2$  for each model. Abbreviations: AD<sub>T</sub>, free-water corrected axial diffusivity; FA<sub>T</sub>, free-water corrected fractional anisotropy; FW, free-water; IFG, inferior frontal gyrus; ILF, inferior longitudinal fasciculus; MD<sub>T</sub>, free-water corrected mean diffusivity; RD<sub>T</sub>, free-water corrected radial diffusivity. Bolded values indicate p-uncorrected < 0.05. \* $p_{FDR} < 0.05$ .

unique variance beyond the base model. Specifically, the inclusion of fornix MD<sub>T</sub>, fornix RD<sub>T</sub>, and IFG pars triangularis RD<sub>T</sub> to the base model results increased the  $R_{adj}^2$  by 5.44%, 5.32%, and 4.06%, respectively.

### 3.4. Multivariate regression to maximize the association with subjective cognitive decline scores

All variables which were nominally significant ( $p < 0.05$ ) in the competitive model analysis, in addition to covariates, were then selected as input variables in a backwards stepwise multiple regression analysis to maximize the  $R_{adj}^2$  value (Fig. 3A). The set of variables which resulted in the best model ( $R_{adj}^2 = 46.69\%$ ;  $p = 6.37 \times 10^{-12}$ ) included ILF  $RD_T$ , fornix  $RD_T$ , UF FW, diagnosis, FSRP score, GDS score, hippocampal volume, and CSF  $A\beta_{42}$  (Fig. 3B). This model increased the  $R_{adj}^2$  by 7.66% compared to the base model (i.e., covariates + CSF  $A\beta_{42}$  only).

## 4. Discussion

The current study leveraged high-resolution white matter tractography templates in conjunction with an advanced diffusion MRI post-processing technique (i.e., FW elimination) to investigate if white matter tract microstructure is associated with SCD. Moreover, we determined if FW-corrected diffusion MRI metrics accounted for significant variance in association with SCD scores beyond that of amyloidosis (CSF  $A\beta_{42}$ ). First, we found that  $RD_T$  showed the most widespread associations with SCD scores, and many of these  $RD_T$  associations explained variance in SCD scores above and beyond CSF  $A\beta_{42}$ . Second, we conducted a multivariate backwards stepwise regression analysis to find the subset of variables which was best associated with SCD scores, and found that these variables included ILF  $RD_T$ , fornix  $RD_T$ , and UF FW (in addition to several well-established covariates). These findings extend prior work reporting associations between multiple diffusion MRI metrics and SCD (Lin et al., 2019; Luo et al., 2019; Ohlhauser et al., 2019; Selnes et al., 2013; Li et al., 2016; Bruggen et al., 2019). Our findings suggest that white matter microstructural values, particularly  $RD_T$ ,

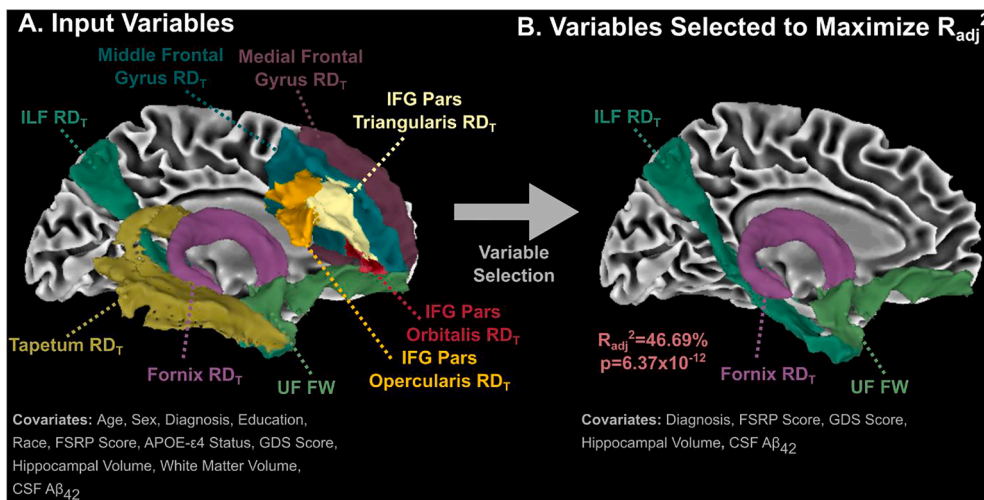


**Fig. 3. Multivariate Association with Subjective Cognitive Decline (SCD).** (A) Tract measures which demonstrated significance in the competitive model (in addition to covariates) were inputted into backwards stepwise multiple regression analysis to maximize the  $R_{adj}^2$ . (B) The set of variables which maximized the  $R_{adj}^2$  included inferior longitudinal fasciculus (ILF)  $RD_T$ , fornix  $RD_T$ , uncinate fasciculus (UF) FW, diagnosis, Framingham Stroke Risk Profile (FSRP) score, Geriatric Depression Score (GDS), hippocampal volume, and CSF  $A\beta_{42}$ .

could have important contributions to SCD that are independent of early AD pathology.

White matter tract integrity is critical for efficient signal propagation between neurons and damage is associated with cognitive disruption; (Ryu et al., 2017; Selnes et al., 2013; DeSimone et al., 2019; Shu et al., 2018) thus, it is not surprising white matter tract abnormalities have been related to SCD (Lin et al., 2019; Luo et al., 2019; Ohlhauser et al., 2019; Selnes et al., 2013; Li et al., 2016; Brueggen et al., 2019). However, this study was among the first to leverage FW correction to evaluate diffusivity metrics, thus providing more sensitive quantification of tissue abnormalities. Using this method, we demonstrated that  $RD_T$  may be a stronger correlate of SCD scores than other intracellular diffusion MRI metrics ( $FA_T$ ,  $AD_T$ ,  $MD_T$ ). Although  $RD_T$  has been implicated in a variety of pathophysiological mechanisms (e.g., demyelination, axonal degeneration, edema) (Winklewski et al., 2018; Song et al., 2003; Song et al., 2005; Kronlage et al., 2017), the prevailing hypothesis is that  $RD_T$  is strongly associated with demyelination. For example, a histological mouse study found that higher radial diffusivity in the corpus callosum was associated with demyelination but not associated with axonal degeneration (Song et al., 2005). While the underlying pathology remains somewhat unclear, our findings demonstrate a clear association between  $RD_T$  and SCD scores in older adults; thus, it's possible that demyelination leads to reduced conduction velocity between critical gray matter regions, ultimately leading to cognitive complaint (Plemel et al., 2017). Future studies which pair *in-vivo* neuroimaging with *post-mortem* histopathological analysis will be pivotal to elucidate the exact pathophysiological mechanisms driving the white matter association with SCD.

The role of white matter tract microstructure in SCD has been investigated in prior studies. The cingulum bundle, forceps major, forceps minor, and ILF are tracts and regions consistently associated with SCD (Luo et al., 2019; Ohlhauser et al., 2019). The current work extends these findings by using FW post-processing techniques and spatially precise templates of cognitive related white matter tracts to implicate several white matter tracts with SCD scores. In our primary analysis, we found widespread  $FA_T$  and  $RD_T$  associations with SCD scores. Following these analyses, we conducted a competitive model analysis in our CSF cohort to find that several tracts contributed unique variance beyond that of CSF  $A\beta_{42}$ . While many tracts demonstrated nominal significance,  $MD_T$  within the fornix and  $RD_T$  within the fornix and IFG pars triangularis demonstrated significance after correction for multiple comparisons. In our final analysis, we input all variables which demonstrated nominal significance (in addition to covariates) into a multivariate regression analysis to optimize the association with SCD scores, and found that  $RD_T$  within the ILF and fornix, in addition to FW within the

UF, were tract measures involved in this model. Consistent with prior work, these analyses implicate several frontal and medial temporal lobe projections with SCD (Ohlhauser et al., 2019). Importantly, these tracts are traditionally associated with executive function, (Stuss and Alexander, 2000) information processing speed, (Kochunov et al., 2010) and memory, (Fujie et al., 2008) so damage in these tracts may contribute to SCD through these cognitive domains. Notably, a secondary analysis (Supplemental Tables 2-4) of SCD subscores (i.e., memory, executive function, language) found that these white matter tract measures were more strongly associated with memory and executive function. Our findings also align with our previous work linking medial temporal lobe tracts to executive function and memory domains of objective cognitive function (Archer et al., 2020). However, further research is needed to better understand the regional and mechanistic specificity of these findings as it is unclear whether SCD is specific to certain tracts and types of white matter damage or rather general white matter injury.

Our findings also suggest that the contribution of white matter microstructure to SCD scores is statistically independent from the contribution of  $A\beta$ . This finding is particularly notable given that  $A\beta$  has been widely associated with SCD (Lin et al., 2019; Selnes et al., 2013; Schoonenboom et al., 2012; Fortea et al., 2011). This finding is consistent with prior work showing that diffusivity metrics are more sensitively associated with cognitive decline and medial temporal lobe atrophy in preclinical AD than CSF  $A\beta$  (Selnes et al., 2013). While the pathological mechanism driving the white matter microstructural changes remains unclear, these results provide further evidence that multiple etiologies contribute to SCD and suggest that FW imaging may be a useful biomarker to more sensitively identify individuals with SCD. Notably, the tracts which provided the most unique variance to SCD scores predominantly project to the frontal lobe, which is highly implicated in episodic memory retrieval and an important contributor to SCD (Barredo et al., 2016; Senova et al., 2020). It is important to note that  $RD_T$  in some tracts (e.g., cingulum bundle) did not contribute unique variance to SCD scores beyond  $A\beta$ , suggesting that alterations in particular tracts could more accurately delineate the etiologies underlying SCD. Future work should examine the specific mechanism underlying these changes and if other forms of white matter injury mediate associations between  $A\beta$  and SCD. Further, models which incorporate both  $A\beta$  and measures of white matter injury should be considered.

In contrast to our widespread findings with  $RD_T$ , there were only subtle associations with  $AD_T$ , suggesting that axonal degeneration may not be a large contributor to SCD (Song et al., 2003). Further, while there were not strong associations with FW, we did find a nominal association of UF FW in our primary analysis as well as involvement in our multivariate regression analysis. FW is a measure which has been consistently



used to evaluate extracellular changes in a variety of neurodegenerative diseases and reflects the unrestricted FW within white matter (Pasternak et al., 2009; Pasternak et al., 2012; Pasternak et al., 2016). It has been suggested to be driven by a variety of pathologies (e.g., neuroinflammation) and is consistently shown to be one of the earliest structural brain changes on the AD continuum (Hoy et al., 2017; Akiyama et al., 2000). Together, our results strongly suggest that RD<sub>T</sub> may be useful as an imaging marker, in addition to A $\beta$  or other molecular biomarkers, to better understand the multiple etiologies underlying SCD (e.g., normal aging, vascular disease, AD pathology). Additionally, our results suggest a potential role of UF FW with SCD. Further research leveraging large-scale neuroimaging data could further clarify the role of these metrics with SCD.

The present study has several strengths. First, we leveraged high-resolution white matter tractography templates of the homologous frontal transcallosal tracts, medial temporal lobe projections, and a parieto-frontal tract. The intention of using these tractography templates is that it makes results more consistent and generalizable across studies. Importantly, these tractography templates are freely available to the public. Second, we paired these tractography templates with the FW post-processing technique, which allowed for the separation of extracellular and intracellular components of the diffusion image. Third, these neuroimaging analysis novelties were leveraged to study SCD scores in the Vanderbilt Memory and Aging Project (VMAP) cohort, which is a well-established longitudinal cohort of aging (Jefferson et al., 2016) with comprehensive covariate collection. Despite these strengths, the VMAP cohort is mostly male, non-Hispanic white and well-educated; therefore, generalizability outside of this population may be limited. Another potential limitation of this study is that it leveraged an ROI-based approach of white matter tracts. It's possible that more comprehensive methods, such as tract-based spatial statistics (TBSS) (Smith et al., 2006), may provide different results. Additionally, only a subset of our cohort (n = 104) had both diffusion MRI and CSF data, thus our analyses using both measures may be underpowered. Finally, the inclusion of multiple comparisons in our study may increase the possibility of false positives, though this was mitigated with false discovery correction. Replication of results in a larger, more diverse cohort is needed to further elucidate the association between white matter tract microstructure and SCD.

In conclusion, this study provided novel evidence that FW-corrected metrics within frontal transcallosal tracts, medial temporal lobe projections, and fronto-parietal tracts are associated with SCD scores, a purported marker of early neurodegenerative changes. Our study found particularly robust associations of FW-corrected radial diffusivity measures on SCD scores, which had unique contributions beyond that of amyloidosis. These findings indicate that early demyelination of white matter is a statistically independent contributor to SCD in older adults. A more robust consideration of both AD pathology and white matter microstructure may help disentangle the mechanistic heterogeneity of SCD as an early stage of cognitive decline.

## 5. Funding acknowledgements

IIRG-08-88733, R01-AG034962, R01-AG059716, K01-AG049164, R01-AG056534, K24-AG046373, F30-AG064847, T32-GM007347, P20-AG068082, K23 AG045966, R01AG062826. KB is supported by the Swedish Research Council (#2017-00915), the Alzheimer Drug Discovery Foundation (ADDF), USA (#RDAPB-201809-2016615), the Swedish Alzheimer Foundation (#AF-742881), Hjärnfonden, Sweden (#FO2017-0243), the Swedish state under the agreement between the Swedish government and the County Councils, the ALF-agreement (#ALFGBG-715986), the European Union Joint Program for Neurodegenerative Disorders (JPND2019-466-236), and the National Institute of Health (NIH), USA, (grant #1R01AG068398-01). HZ is a Wallenberg Scholar supported by grants from the Swedish Research Council (#2018-02532), the European Research Council (#681712), Swedish

State Support for Clinical Research (#ALFGBG-720931), the Alzheimer Drug Discovery Foundation (ADDF), USA (#201809-2016862), the AD Strategic Fund and the Alzheimer's Association (#ADSF-21-831376-C, #ADSF-21-831381-C and #ADSF-21-831377-C), the Olav Thon Foundation, the Erling-Persson Family Foundation, Stiftelsen för Gamla Tjänarinnor, Hjärnfonden, Sweden (#FO2019-0228), the European Union's Horizon 2020 research and innovation programme under the Marie Skłodowska-Curie grant agreement No 860,197 (MIRIADE), and the UK Dementia Research Institute at UCL.

## 6. Disclosure Statement

KB has served as a consultant, at advisory boards, or at data monitoring committees for Abcam, Axon, Biogen, JOMDD/Shimadzu. Julius Clinical, Lilly, MagQu, Novartis, Roche Diagnostics, and Siemens Healthineers, and is a co-founder of Brain Biomarker Solutions in Gothenburg AB (BBS), which is a part of the GU Ventures Incubator Program, all outside the submitted work. HZ has served at scientific advisory boards for Eisai, Denali, Roche Diagnostics, Wave, Samumed, Siemens Healthineers, Pinteon Therapeutics, Nervgen, AZTherapies and CogRx, has given lectures in symposia sponsored by Cellectricon, Fujirebio, Alzecure and Biogen, and is a co-founder of Brain Biomarker Solutions in Gothenburg AB (BBS), which is a part of the GU Ventures Incubator Program (outside submitted work). The other authors report a conflict of interest relevant to this research.

## CRedit authorship contribution statement

**Derek B. Archer:** Conceptualization, Methodology, Software, Validation, Formal analysis, Investigation, Writing - original draft, Writing - review & editing, Visualization. **Elizabeth E. Moore:** Validation, Writing - original draft, Writing - review & editing. **Ujwala Pamidimukkala:** Writing - original draft, Writing - review & editing. **Niranjana Shashikumar:** Methodology, Software, Validation, Data curation, Writing - review & editing. **Kimberly R. Pechman:** Data curation, Writing - review & editing. **Kaj Blennow:** Writing - review & editing. **Henrik Zetterberg:** Resources, Writing - review & editing. **Bennett A. Landman:** Writing - review & editing. **Timothy J. Hohman:** Resources, Writing - review & editing, Supervision, Funding acquisition. **Angela L. Jefferson:** Resources, Writing - review & editing, Supervision, Project administration, Funding acquisition. **Katherine A. Gifford:** Conceptualization, Methodology, Resources, Writing - original draft, Writing - review & editing, Supervision, Funding acquisition.

## Appendix A. Supplementary data

Supplementary data to this article can be found online at <https://doi.org/10.1016/j.nicl.2021.102794>.

## References

- Akiyama, H., Barger, S., Barnum, S., et al., 2000. Inflammation and Alzheimer's disease. *Neurobiol. Aging* 21 (3), 383–421.
- Albert, M.S., DeKosky, S.T., Dickson, D., Phelps, C.H., et al., 2011. The diagnosis of mild cognitive impairment due to Alzheimer's disease: recommendations from the National Institute on Aging-Alzheimer's Association workgroups on diagnostic guidelines for Alzheimer's disease. *Alzheimer's Dementia* 7 (3), 270–279.
- Alexander, A.L., Hasan, K.M., Lazar, M., Tsuruda, J.S., Parker, D.L., 2001. Analysis of partial volume effects in diffusion-tensor MRI. *Magn. Reson. Med.* 45 (5), 770–780.
- Andersson, J.L.R., Sotiropoulos, S.N., 2016. An integrated approach to correction for off-resonance effects and subject movement in diffusion MR imaging. *NeuroImage* 125, 1063–1078.
- Archer, D.B., Coombes, S.A., McFarland, N.R., DeKosky, S.T., Vaillancourt, D.E., 2019. Development of a transcallosal tractography template and its application to dementia. *NeuroImage* 200, 302–312.
- Archer, D.B., Bricker, J.T., Chu, W.T., et al., 2019. Development and validation of the automated imaging differentiation in parkinsonism (AID-P): a multicentre machine learning study. *The Lancet Digital Health* 1 (5), e222–e231.



- Archer, D.B., Moore, E.E., Shashikumar, N., et al., 2020. Free-water metrics in medial temporal lobe white matter tract projections relate to longitudinal cognitive decline. *Neurobiol. Aging* 94, 15–23.
- Avants, B., Epstein, C., Grossman, M., Gee, J., 2008. Symmetric diffeomorphic image registration with cross-correlation: Evaluating automated labeling of elderly and neurodegenerative brain. *Med. Image Anal.* 12 (1), 26–41.
- Barredo, J., Verstynen, T.D., Badre, D., 2016. Organization of cortico-cortical pathways supporting memory retrieval across subregions of the left ventrolateral prefrontal cortex. *J. Neurophysiol.* 116 (3), 920–937.
- Bartzokis, G., 2011. Alzheimer's disease as homeostatic responses to age-related myelin breakdown. *Neurobiol. Aging* 32 (8), 1341–1371.
- Brown, C.A., Johnson, N.F., Anderson-Mooney, A.J., et al., 2017. Development, validation and application of a new fornix template for studies of aging and preclinical Alzheimer's disease. *NeuroImage: Clinical* 13, 106–115.
- Brueggen, K., Dyrba, M., Cardenas-Blanco, A., et al., 2019. Structural integrity in subjective cognitive decline, mild cognitive impairment and Alzheimer's disease based on multicenter diffusion tensor imaging. *J. Neurol.* 266 (10), 2465–2474.
- Cherbuin, N., Sargent-Cox, K., Easteal, S., Sachdev, P., Anstey, K.J., 2015. Hippocampal atrophy is associated with subjective memory decline: The PATH through life study. *Am. J. Geriatric Psychiatry* 23 (5), 446–455.
- Crook, D.M.J., 1983 *Self-assessment of cognitive deficits*. Mark Powley Associates Inc; 1983.
- D'Agostino, R.B., Wolf, P.A., Belanger, A.J., Kannel, W.B., 1994. Stroke risk profile: adjustment for antihypertensive medication. *The Framingham Study. Stroke* 25 (1), 40–43.
- de Groot, M., Ikram, M.A., Akoudad, S., et al., 2015. Tract-specific white matter degeneration in aging: the Rotterdam Study. *Alzheimer's Dementia* 11 (3), 321–330.
- DeSimone, J.C., Archer, D.B., Vaillancourt, D.E., Wagle Shukla, A., 2019. Network-level connectivity is a critical feature distinguishing dystonic tremor and essential tremor. *Brain*. 142(6):1644-1659.
- Farias, S.T., Mungas, D., Reed, B.R., et al., 2008. The measurement of everyday cognition (ECog): scale development and psychometric properties. *Neuropsychology* 22(4): 531-544.
- Fortea, J., Sala-Llonch, R., Bartres-Faz, D., et al., 2011. Cognitively preserved subjects with transitional cerebrospinal fluid ss-amyloid 1–42 values have thicker cortex in Alzheimer's disease vulnerable areas. *Biol. Psychiatry* 70 (2), 183–190.
- Fujie, S., Namiki, C., Nishi, H., et al., 2008. The role of the uncinate fasciculus in memory and emotional recognition in amnesic mild cognitive impairment. *Dement Geriatr. Cogn. Disord.* 26 (5), 432–439.
- Gifford, K.A., Liu, D., Lu, Z., et al., 2014. The source of cognitive complaints predicts diagnostic conversion differentially among nondemented older adults. *Alzheimer's Dementia* 10 (3), 319–327.
- Gifford, K.A., Liu, D., Carmona, H., et al., 2014. Inclusion of an informant yields strong associations between cognitive complaint and longitudinal cognitive outcomes in non-demented elders. *JAD* 43 (1), 121–132.
- Gifford, K.A., Liu, D., Romano III, R.R., Jones, R.N., Jefferson, A.L., 2015. Development of a subjective cognitive decline questionnaire using item response theory: A pilot study. *Alzheimer's Dementia (Amst)* 1 (4), 429–439.
- Gilewski, M.J., Zelinski, E.M., Schaie, K.W., 1990. The Memory Functioning Questionnaire for assessment of memory complaints in adulthood and old age. *Psychol Aging* 5(4):482-490.
- Gullett, J.M., O'Shea, A., Lamb, D.G., Porges, E.C., O'Shea, D.M., Pasternak, O., Cohen, R.A., Woods, A.J., 2020. The association of white matter free water with cognition in older adults. *NeuroImage* 219, 117040.
- Hoy, A.R., Ly, M., Carlsson, C.M., et al., 2017. Microstructural white matter alterations in preclinical Alzheimer's disease detected using free water elimination diffusion tensor imaging. *PLoS ONE* 12 (3), e0173982.
- Jefferson, A.L., Gifford, K.A., Acosta, L.M.Y., et al., 2016. The Vanderbilt Memory & Aging Project: Study Design and Baseline Cohort Overview. *Journal of Alzheimer's Disease*. (Preprint):1-20.
- Jenkinson, M., Beckmann, C.F., Behrens, T.E.J., Woolrich, M.W., Smith, S.M., 2012. FSL. *NeuroImage* 62 (2), 782–790.
- Jessen, F., Amariglio, R.E., van Boxtel, M., et al., 2014. A conceptual framework for research on subjective cognitive decline in preclinical Alzheimer's disease. *Alzheimer's Dementia* 10 (6), 844–852.
- Jones, D.K., Knösche, T.R., Turner, R., 2013. White matter integrity, fiber count, and other fallacies: The do's and don'ts of diffusion MRI. *NeuroImage* 73, 239–254.
- Kochunov, P., Coyle, T., Lancaster, J., et al., 2010. Processing speed is correlated with cerebral health markers in the frontal lobes as quantified by neuroimaging. *NeuroImage* 49 (2), 1190–1199.
- Kronlage, M., Pitarokouli, K., Schwarz, D., Godel, T., Heiland, S., Yoon, M.-S., Bendszus, M., Bäumer, P., 2017. Diffusion tensor imaging in chronic inflammatory demyelinating polyneuropathy: diagnostic accuracy and correlation with electrophysiology. *Invest. Radiol.* 52 (11), 701–707.
- Li, X.-y., Tang, Z.-C., Sun, Y.-u., Tian, J., Liu, Z.-y., Han, Y., 2016. White matter degeneration in subjective cognitive decline: a diffusion tensor imaging study. *Oncotarget* 7 (34), 54405–54414.
- Lin, Y., Shan, P.-Y., Jiang, W.-J., Sheng, C., Ma, L., 2019. Subjective cognitive decline: preclinical manifestation of Alzheimer's disease. *Neurol. Sci.* 40 (1), 41–49.
- Luo, C., Li, M., Qin, R., et al., 2019. White Matter Microstructural Damage as an Early Sign of Subjective Cognitive Decline. *Front Aging Neurosci* 11:378.
- Meiberth, D., Scheef, L., Wolfsgruber, S., et al., 2015. Cortical Thinning in Individuals with Subjective Memory Impairment. *JAD* 45 (1), 139–146.
- Metzler-Baddeley, C., Mole, J.P., Sims, R., et al., 2019. Fornix white matter glia damage causes hippocampal gray matter damage during age-dependent limbic decline. *Sci. Rep.* 9 (1), 1060.
- Morris, J.C., 1993. The Clinical Dementia Rating (CDR): current version and scoring rules. *Neurology* 43(11):2412-2414.
- Ohlhauser, L., Parker, A.F., Smart, C.M., Gawryluk, J.R., 2019. White matter and its relationship with cognition in subjective cognitive decline. *Alzheimer's Dement (Amst)* 11, 28–35.
- Osborn, K.E., Liu, D., Samuels, L.R., et al., 2018. Cerebrospinal fluid  $\beta$ -amyloid42 and neurofilament light relate to white matter hyperintensities. *Neurobiol. Aging* 68, 18–25.
- Palmqvist, S., Zetterberg, H., Blennow, K., et al., 2014. Accuracy of brain amyloid detection in clinical practice using cerebrospinal fluid beta-amyloid 42: a cross-validation study against amyloid positron emission tomography. *JAMA Neurol.* 71 (10), 1282–1289.
- Pasternak, O., Sochen, N., Gur, Y., Intrator, N., Assaf, Y., 2009. Free water elimination and mapping from diffusion MRI. *Magn. Reson. Med.* 62 (3), 717–730.
- Pasternak, O., Westin, C.-F., Bouix, S., et al., 2012. Excessive extracellular volume reveals a neurodegenerative pattern in schizophrenia onset. *J. Neurosci.* 32 (48), 17365–17372.
- Pasternak, O., Kubicki, M., Shenton, M.E., 2016. In vivo imaging of neuroinflammation in schizophrenia. *Schizophr. Res.* 173 (3), 200–212.
- Perrotin, A., La Joie, R., de La Sayette, V., et al., 2017. Subjective cognitive decline in cognitively normal elders from the community or from a memory clinic: differential affective and imaging correlates. *Alzheimer's Dementia* 13 (5), 550–560.
- Pfeffer, R.I., Kurosaki, T.T., Harrah, C.H., Chance, J.M., Filos, S., 1982. Measurement of functional activities in older adults in the community. *J. Gerontol.* 37 (3), 323–329.
- Plemel, J.R., Liu, W.-Q., Yong, V.W., 2017. Remyelination therapies: a new direction and challenge in multiple sclerosis. *Nat. Rev. Drug Discov.* 16 (9), 617–634.
- Reid, L.M., MacLulich, A.M., 2006. Subjective memory complaints and cognitive impairment in older people. *Dement Geriatr Cogn Disord.* 22(5-6):471-485.
- Ryu, S.Y., Lim, E.Y., Na, S., et al., 2017. Hippocampal and entorhinal structures in subjective memory impairment: a combined MRI volumetric and DTI study. *Int. Psychogeriatr.* 29 (5), 785–792.
- Sachdev, P.S., Zhuang, L., Braidy, N., Wen, W., 2013. Is Alzheimer's a disease of the white matter? *Current opinion in psychiatry.* 26(3):244-251.
- Schoonenboom, N.S.M., Reesink, F.E., Verwey, N.A., et al., 2012. Cerebrospinal fluid markers for differential dementia diagnosis in a large memory clinic cohort. *Neurology* 78 (1), 47–54.
- Selnes, P., Aarsland, D., Bjørnerud, A., et al., 2013. Diffusion tensor imaging surpasses cerebrospinal fluid as predictor of cognitive decline and medial temporal lobe atrophy in subjective cognitive impairment and mild cognitive impairment. *JAD* 33 (3), 723–736.
- Senova, S., Fomenko, A., Gondard, E., Lozano, A.M., 2020. Anatomy and function of the fornix in the context of its potential as a therapeutic target. *J. Neurol. Neurosurg. Psychiatry* 91 (5), 547–559.
- Shu, N.i., Wang, X., Bi, Q., Zhao, T., Han, Y., 2018. Disrupted topologic efficiency of white matter structural connectome in individuals with subjective cognitive decline. *Radiology* 286 (1), 229–238.
- Smith, S.M., 2002. Fast robust automated brain extraction. *Hum. Brain Mapp.* 17 (3), 143–155.
- Smith, S.M., Jenkinson, M., Johansen-Berg, H., et al., 2006. Tract-based spatial statistics: Voxelwise analysis of multi-subject diffusion data. *NeuroImage* 31 (4), 1487–1505.
- Song, S.-K., Sun, S.-W., Ju, W.-K., Lin, S.-J., Cross, A.H., Neufeld, A.H., 2003. Diffusion tensor imaging detects and differentiates axon and myelin degeneration in mouse optic nerve after retinal ischemia. *NeuroImage* 20 (3), 1714–1722.
- Song, S.-K., Yoshino, J., Le, T.Q., et al., 2005. Demyelination increases radial diffusivity in corpus callosum of mouse brain. *NeuroImage* 26 (1), 132–140.
- Sperling, R.A., Aisen, P.S., Beckett, L.A., et al., 2011. Toward defining the preclinical stages of Alzheimer's disease: Recommendations from the National Institute on Aging-Alzheimer's Association workgroups on diagnostic guidelines for Alzheimer's disease. *Alzheimer's Dementia* 7 (3), 280–292.
- Stomrud, E., Hansson, O., Blennow, K., Minthon, L., Londos, E., 2007. Cerebrospinal fluid biomarkers predict decline in subjective cognitive function over 3 years in healthy elderly. *Dement Geriatr Cogn Disord.* 24(2):118-124.
- Stuss, D.T., Alexander, M.P., 2000. Executive functions and the frontal lobes: a conceptual view. *Psychol. Res.* 63 (3-4), 289–298.
- van der Flier, W.M., van Buchem, M.A., Weverling-Rijnsburger, A.W., et al., 2004. Memory complaints in patients with normal cognition are associated with smaller hippocampal volumes. *J. Neurol.* 251 (6), 671–675.
- Verfaillie, S.C.J., Slot, R.E., Tijms, B.M., et al., 2018. Thinner cortex in patients with subjective cognitive decline is associated with steeper decline of memory. *Neurobiol. Aging* 61, 238–244.
- Verfaillie, S.C.J., Timmers, T., Slot, R.E.R., et al., 2019. Amyloid-beta Load Is related to worries, but not to severity of cognitive complaints in individuals with subjective cognitive decline: The SCIENCE Project. *Front Aging Neurosci.* 11, 7.
- Walsh, R., Bergamino, M., Stokes, A., 2020. Free-water diffusion tensor imaging (DTI) improves the accuracy and sensitivity of white matter analysis in Alzheimer's Disease (4979). *Neurology* 94.
- Winklewski, P.J., Sabitz, A., Naumczyk, P., Jodzio, K., Szurowska, E., Szarmach, A., 2018. Understanding the physiopathology behind axial and radial diffusivity changes-what do we know? *Front Neurol.* 9, 92.
- Wolf, P.A., D'Agostino, R.B., Belanger, A.J., Kannel, W.B., 1991. Probability of stroke: a risk profile from the Framingham Study. *Stroke* 22 (3), 312–318.
- Wolfsgruber, S., Jessen, F., Koppa, A., et al., 2015. Subjective cognitive decline is related to CSF biomarkers of AD in patients with MCI. *Neurology* 84 (12), 1261–1268.
- Yesavage, J.A., 1988. Geriatric depression scale. *Psychopharmacol. Bull.* 24 (4), 709–711.